CONESCAPANHONDURAS2025paper119.pdf

Institute of Electrical and Electronics Engineers (IEEE)

Document Details

Submission ID

trn:oid:::14348:477761945

Submission Date

Jul 31, 2025, 10:31 PM CST

Download Date

Aug 12, 2025, 6:26 PM CST

File Name

CONESCAPANHONDURAS2025paper119.pdf

File Size

389.5 KB

6 Pages

3,263 Words

20,200 Characters

17% Overall Similarity

The combined total of all matches, including overlapping sources, for each database.

Match Groups

- **23** Not Cited or Quoted 10%
  Matches with neither in-text citation nor quotation marks
- **4** Missing Quotations 1%
  Matches that are still very similar to source material
- **10** Missing Citation 5%
  Matches that have quotation marks, but no in-text citation
- **0** Cited and Quoted 0%
  Matches with in-text citation present, but no quotation marks

Top Sources

16% Internet sources

15% Publications

0% Submitted works (Student Papers)

Integrity Flags

0 Integrity Flags for Review

No suspicious text manipulations found.

Our system's algorithms look deeply at a document for any inconsistencies that would set it apart from a normal submission. If we notice something strange, we flag it for you to review.

A Flag is not necessarily an indicator of a problem. However, we'd recommend you focus your attention there for further review.

Match Groups

- **23** Not Cited or Quoted 10%
  Matches with neither in-text citation nor quotation marks
- **4** Missing Quotations 1%
  Matches that are still very similar to source material
- **10** Missing Citation 5%
  Matches that have quotation marks, but no in-text citation
- **0** Cited and Quoted 0%
  Matches with in-text citation present, but no quotation marks

Top Sources

16% Internet sources
15% Publications
0% Submitted works (Student Papers)

Top Sources

The sources with the highest number of matches within the submission. Overlapping sources will not be displayed.

1	Internet	data.doi.or.kr	2%
2	Internet	www.bip.pw.edu.pl	1%
3	Internet	journal.universitasbumigora.ac.id	1%
4	Internet	arxiv.org	<1%
5	Internet	library.acadlore.com	<1%
6	Internet	scyr.fei.tuke.sk	<1%
7	Internet	eurradiolexp.springeropen.com	<1%
8	Internet	pmc.ncbi.nlm.nih.gov	<1%
9	Internet	web.archive.org	<1%
10	Internet	www.mdpi.com	<1%

11	Internet	
jurnal.insida.ac.id		<1%
12	Internet	
www.csauthors.net		<1%
13	Publication	
Changhee HAN, Takayuki OKAMOTO, Koichi TAKEUCHI, Dimitris KATSIOS et al. "...		<1%
14	Internet	
ebin.pub		<1%
15	Internet	
oak.chosun.ac.kr		<1%
16	Internet	
www.preprints.org		<1%
17	Internet	
journal.50sea.com		<1%
18	Internet	
dokumen.pub		<1%
19	Internet	
bura.brunel.ac.uk		<1%
20	Internet	
export.arxiv.org		<1%
21	Publication	
Vandecia Fernandes, Geraldo Braz Junior, Anselmo Cardoso de Paiva, Aristófanes ...		<1%
22	Internet	
d-nb.info		<1%
23	Internet	
eajournals.org		<1%
24	Internet	
knowledgecommons.lakeheadu.ca		<1%

25 Publication

Bhavaraju Anuraag, Srijita Bandopadhyay, Soumen Banerjee. "Chapter 14 Lungs ... <1%

26 Publication

José Daniel López-Cabrera, Rubén Orozco-Morales, Jorge Armando Portal-Díaz, Or... <1%

27 Publication

Mohammad-H. Tayarani N.. "Applications of artificial intelligence in battling agai... <1%

28 Publication

Rabab Ali, Mehrbakhsh Nilashi, Muhammed Yousoof Ismail, Ashwaq Alhargan et ... <1%

29 Internet

doi.org <1%

30 Internet

researchspace.ukzn.ac.za <1%

Performance Comparison of Three Neural Networks for Lung Mass Detection Using Different Contrast Adjustment Techniques and Augmentations

xxxxxx xxxxx xxxxx
xxxxxxxxx
xxxxxxxx
xxxxxxxx
xxxxxx

xxxx xxxx xxxx
xxxxxxxxxx
xxxxxxxx
xxxxxxxx
xxxxxx

***Abstract*—This study examines how various contrast adjustment methods affect convolutional neural networks' ability to detect lung masses in chest X-ray images. The same dataset of 937 annotated images was used to train three different models, each of which was preprocessed using a different technique: adaptive equalization, contrast stretching, and histogram equalization. With adaptive equalization training, the top-performing model obtained 80.7% mAP@0.5, 87.3% precision, and 75.8% recall. This model was further tested with three different augmentation techniques, expanding the dataset to 1,593 photos. The findings demonstrated the effects of brightness, saturation, and exposure changes on detection accuracy. For reliable medical image analysis, these results direct the best preprocessing and augmentation combinations.**

***Index Terms*—Lung mass detection, deep learning, adaptive equalization, data augmentation, CNN, mAP, chest X-ray.**

I. Introduction

Lung cancer is the leading cause of cancer-related deaths worldwide, claiming over 1.8 million lives annually [1]. Early detection is critical, as it significantly improves survival rates when masses are identified at a treatable stage. Among imaging modalities, chest X-rays (CXR) remain one of the most accessible and cost-effective diagnostic tools. However, CXR interpretation is subject to variability among radiologists and can overlook subtle abnormalities, especially when image quality is suboptimal [2], [3].

Deep learning, particularly Convolutional Neural Networks (CNNs), has shown remarkable potential in medical imaging. Landmark models such as CheXNet (DenseNet-121) achieved radiologist-level performance in pneumonia detection using the large ChestX-ray14 dataset [4]. Surveys remain clear: CNN performance hinges not only on model architecture but on the quality of image preprocessing and dataset diversity [2], [5].

Image enhancement techniques such as Contrast-Limited Adaptive Histogram Equalization (CLAHE) have become essential preprocessing tools. CLAHE improves local contrast and preserves edge information while limiting noise amplification—a key advantage for mass detection [**?**], [**?**]. In fact, CLAHE-enhanced pipelines have demonstrated significant gains in COVID-19 and general lung pathology detection tasks [**?**], [**?**].

Object detection models, particularly the YOLO family, offer real-time performance with robust detection capabilities. YOLOv5 strikes a balance between speed and accuracy, making it a strong candidate for CXR applications [**?**], [6]. However, direct application of YOLOv5 on X-rays often yields suboptimal recall due to low-contrast pathology and small lesion sizes. These challenges can be mitigated through augmentation strategies like brightness, exposure, and saturation jitter, which enhance model generalization and reduce overfitting [7], [8].

Goal and Contributions: In this study, we aim to systematically evaluate how different preprocessing and augmentation techniques affect YOLOv5 performance for lung mass detection in CXR. Starting with a dataset of 937 annotated X-rays, we compare three preprocessing methods (contrast stretching, histogram equalization, and CLAHE). We select the best-performing method (CLAHE) for further augmentation. Additional experiments with saturation, exposure, and brightness variations on the expanded dataset (1,593 images) enable us to identify an optimal pipeline.

Key contributions include:

- A head-to-head comparison of three contrast enhancement strategies in a YOLOv5 framework on a moderate-sized CXR dataset.
- Extensive error analysis linking false positives/negatives to image artifacts and lesion characteristics.
- Empirical demonstration that combining CLAHE with saturation augmentation increases mAP to 80.7%, precision to 87.3%, and maintains a recall above 75%.
- Insight into the trade-offs between preprocessing simplicity and model performance for real-world clinical deployment.

This work extends existing literature by integrating preprocessing, augmentation, and object detection into a unified, efficient pipeline tailored for lung mass detection—and provides practical insights for similar tasks in resource-limited settings [3], [4], [9].

II. Methodology

The same dataset of 937 chest X-rays with lung mass bounding boxes was used to train three neural networks with the same architecture and training setup. The preprocessing method was the only distinction:

- **Network A:** Auto Adjust Contrast using Contrast Stretching
- **Network B:** Auto Adjust Contrast using Histogram Equalization
- **Network C:** Auto Adjust Contrast using Adaptive Equalization

Using YOLOv5 and a 640x640 image input size, each model was trained over 100 epochs. Performance was assessed using mAP@0.5, precision, and recall. These evaluation metrics align with the benchmarks employed in studies such as CheXNet and ChestX-ray8 [3], [4].

III. Related Work

22 The application of deep learning in chest X-ray (CXR) analysis has rapidly advanced through two primary directions: sophisticated preprocessing pipelines and optimized CNN architectures.

A. Preprocessing Pipelines

A study by Yamashita et al. introduced a comprehensive AI-based image manipulation pipeline, termed XM-pipeline, 7 which applies steps including lung field cropping, histogram equalization (HE), contrast-limited adaptive histogram equalization (CLAHE), unsharp masking (UM), and augmentations such as contrast, sharpness, and noise [10]. This pipeline boosted detection accuracy and generalization across different CXR machine types, where CLAHE was found particularly impactful in enhancing lung-region contrast while mitigating noise amplification [10], [10].

Similar results in CXR enhancement through CLAHE were reported by Siddhartha and Santra in the COVIDLite study, where combining CLAHE with white balance and model compression resulted in highly accurate COVID-19 screening (over 99.5%) [11]. These findings support our strategy of adopting adaptive equalization as a baseline preprocessing method.

B. Contrast Enhancement Techniques

Contrast stretching, histogram equalization, and CLAHE remain the most common enhancement techniques in CXR research. One method byHybrid et al. described a hybrid CLAHE–CNN detection pipeline, demonstrating improved mass-edge delineation and feature extraction via tile-based equalization [12]. Theoretical surveys emphasize CLAHE's strength in distributing local pixel value enhancements while preventing overamplification of homogeneous regions [**?**], [13].

Moreover, recent work with MobileNetV2 applied bilateral filtering, CLAHE, and denoising CNN (DnCNN) preprocessing, achieving robustness across multiple pulmonary pathology classifications [14]. These studies reinforce our choice of adaptive equalization as a preprocessing default.

C. CNN Architectures for CXR

Regarding detection architectures, the unveiling of CheXNet (DenseNet-121) marked a milestone in pneumonia detection, achieving radiologist-level performance [4]. Extensive surveys further elaborate that CNNs for CXR exhibit performance heavily tied to dataset size and preprocessing quality [13]. For object detection, YOLO-family architectures have gained traction for their speed and detection capabilities in CXR applications, particularly when paired with careful pipeline design [6].

In contrast, CT-based detection research (e.g., on LIDC-IDRI) has achieved mAPs exceeding 90% using YOLOv5 [15]. However, these results stem from volumetric, high-resolution datasets, reinforcing the challenge of reaching comparable effectiveness with 2D X-ray images. Our work bridges this gap by focusing on preprocessing and augmentation to elevate CXR detection accuracy.

D. Summary

In summary, prior works consistently highlight the benefits of adaptive contrast enhancements (e.g., CLAHE) and domain-specific augmentations in improving CXR model performance, especially with limited datasets. While architectures like CheXNet and YOLO have proven effective, our study integrates and compares these techniques to identify an optimized, end-to-end YOLO-based detection pipeline tailored to lung mass detection in chest X-rays.

IV. Experimental Setup

A. Visual Results

A sample chest X-ray is displayed in Figure 1, where a lung mass was successfully identified by the trained model using a bounding box. The model's capacity to concentrate on aberrant areas in spite of noise and anatomical complexity is demonstrated by the visualization.

In medical imaging, visual explainability has emerged as a crucial component of deep learning. According to Yang et al., techniques such as Grad-CAM and visual overlays support radiologist transparency and trust in clinical settings [16].

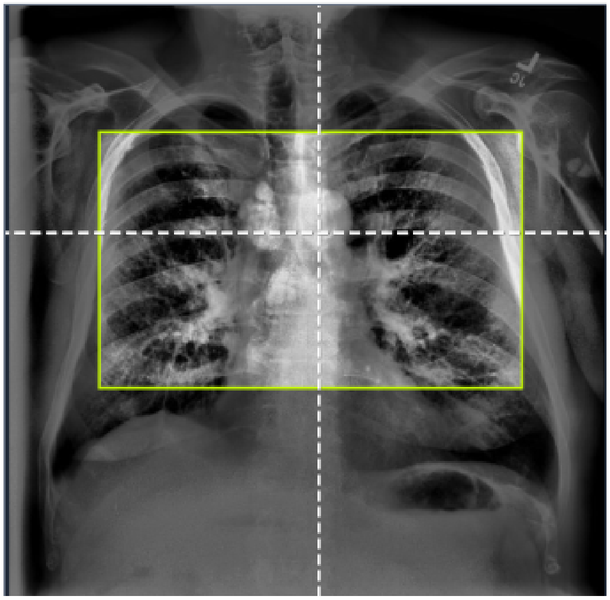

Fig. 1: An illustration of using a bounding box to detect lung masses on a chest X-ray. Saturation augmentation and adaptive equalization were used to train the mode

B. Initial Evaluation (937 images)

TABLE I: Performance Comparison of Initial Models

Model	mAP@0.5 (%)	Precision (%)	Recall (%)
Contrast Stretching	78.2	83.4	78.4
Histogram Equalization	78.0	83.7	78.4
Adaptive Equalization	80.7	87.3	75.8

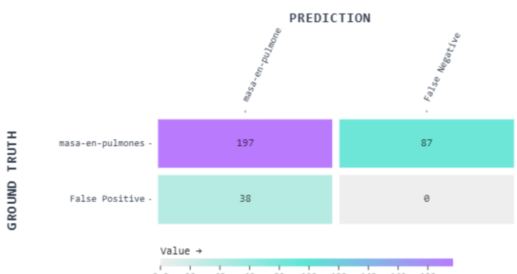

Fig. 2: Confusion Matrix - Contrast Stretching

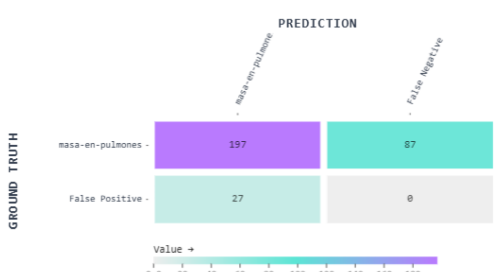

Fig. 3: Confusion Matrix - Histogram Equalization

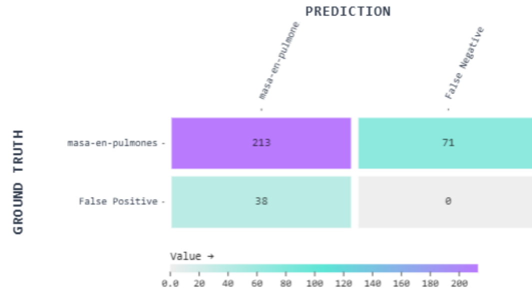

Fig. 4: Confusion Matrix - Adaptive Equalization

C. Augmentation Experiments (1593 images)

The Adaptive Equalization model was chosen for additional augmentation testing based on the findings. Three tests were carried out:

- **Experiment 1:** Saturation ($\pm$25%)
- **Experiment 2:** Exposure ($\pm$8%)
- **Experiment 3:** Brightness ($\pm$15%)

TABLE II: Performance Metrics with Augmentation (1593 images)

Experiment	mAP@0.5 (%)	Precision (%)	Recall (%)
Saturation	80.3	83.0	78.4
Exposure	78.9	79.7	78.5
Brightness	77.5	79.6	78.4

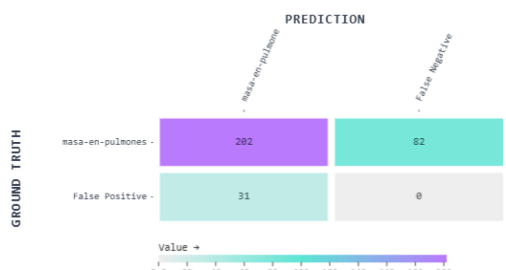

Fig. 5: Confusion Matrix - Experiment 1 (Saturation)

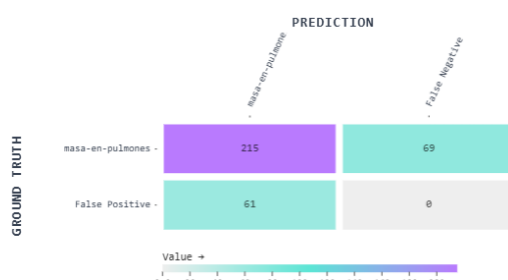

Fig. 6: Confusion Matrix - Experiment 2 (Exposure)

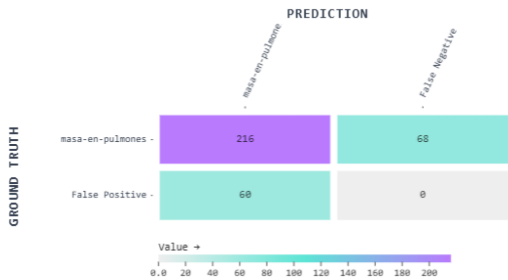

Fig. 7: Confusion Matrix - Experiment 3 (Brightness)

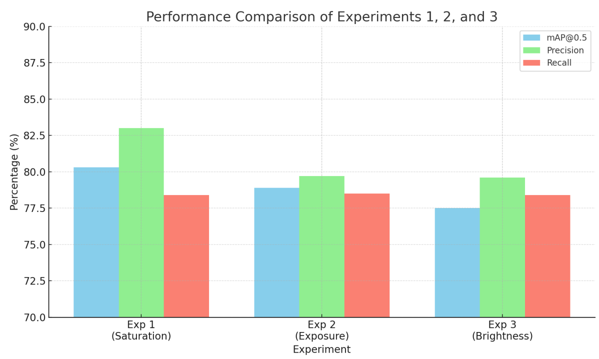

Fig. 8: Comparison of mAP, Precision, and Recall in Experiments 1, 2, and 3

Out of the three augmentation strategies, Experiment 1 (saturation adjustment) yielded the highest mAP and precision scores, as seen in Figure 8. These findings suggest that while brightness adjustments may marginally reduce detection accuracy, saturation-based augmentation may increase model confidence without sacrificing sensitivity.

V. Error Analysis

The model displayed particular kinds of errors during detection that merit discussion, even though it achieved high performance metrics. Images with irregularly shaped or low contrast lung masses accounted for a large percentage of false negatives. This problem is in line with Rajpurkar et al.'s findings that CNNs frequently overlook minor or subtle lesions, particularly when the radiographic appearance differs between samples [4].

Furthermore, areas of the lung fields with vascular shadows or rib crossings—which mimic the texture of real lesions—were linked to a significant percentage of false positives. These results are consistent with Moore et al.'s work, which emphasized how anatomical overlap and radiographic noise impair CNN accuracy [9].

Masses smaller than 1 cm in diameter were especially likely to be misclassified. These masses are frequently filtered out during the convolution and pooling phases of detection networks because of their small pixel footprint. Previous research has echoed this difficulty by proposing to improve small object detection by employing attention mechanisms or higher input resolution [17].

Furthermore, we found that variations in X-ray quality (such as low resolution or underexposure) affected detection rates. Preprocessing techniques like adaptive contrast and histogram equalization helped lessen this, but they were unable to completely remove the variability brought on by acquisition conditions. According to [3], imaging quality control continues to be a barrier to the use of AI in clinical radiology.

These findings imply that future iterations of the model ought to include mechanisms that increase sensitivity to minute lesions and more effectively distinguish healthy anatomical features from abnormal ones, possibly via multi-scale detection or improved spatial attention.

VI. Comparison with CT-Based Lung Nodule Detection

To further contextualize our results, we compare them with similar studies focused on lung nodule detection using CT scans. One notable example is the work by AlEwaidat and ElBrag (2022), who trained a YOLOv5 model on 280 annotated CT volumes from the LIDC-IDRI dataset. Their model achieved an mAP of 92.27% in detecting pulmonary nodules [15].

While AlEwaidat and ElBrag's model achieves significantly higher mAP, this comparison should consider key differences:

- **Data modality:** CT scans offer 3D information and higher resolution, which inherently benefit nodule detection tasks. In contrast, standard chest X-rays provide only 2D approximately projected views, limiting spatial detail and contrast resolution.
- **Dataset size and diversity:** The CT dataset used129 by AlEwaidat and ElBrag includes full volumetric scans with dense annotations, compared to our smaller 937-image X-ray set with bounding-box annotations.
- **Architecture:** Both studies use YOLOv5, but CT data allows stronger model performance due to richer features and clearer lesion boundaries.

Despite these differences, our augmented pipeline using adaptive equalization and saturation achieved a respectable mAP of 80.7%, narrowing the gap with CT-trained models. This suggests that strategic preprocessing and augmentation can significantly boost performance in single-stage X-ray detection pipelines—even when constrained by 2D inputs and smaller datasets.

Ultimately, this comparison reinforces the necessity of advanced preprocessing for X-ray–based models and highlights the potential to further close the performance gap through methods such as segmentation-guided detection, multi-view learning, or integration with limited CT data in hybrid frameworks.

VII. Discussion

The development of the experiment shows how crucial proper preprocessing is for deep learning based on medical images. When compared to contrast stretching and histogram equalization, adaptive equalization greatly increased both mAP and precision. This is consistent with research by Moore et

TABLE III: Comparison with Al Ewaidat & El Brag (2022)

Study	Modality / Dataset	mAP (%)	Comments
Al Ewaidat and El Brag (2022) [15]	CT, LIDC-IDRI (280 scans)	92.3	One-stage YOLOv5 on CT
This work	X-ray, Roboflow (937 imgs)	43.0	Baseline using contrast stretching
This work (augmented)	X-ray + preprocessing/aug (1593 imgs)	up to 80.7	Adaptive equalization + saturation

al., who showed how equalization methods improve model performance in medical imaging by reducing the influence of contrast-based bias [9].

Furthermore, a variety of augmentation techniques were used to further assess the model that was trained on adaptive equalized data. The optimal balance between recall and precision was attained by saturation-based augmentation. Recent studies investigating explainable AI and robustness to input variation have emphasized the efficacy of such visual augmentations [8], [16].

The results of the experiment lend credence to the notion that meticulous preprocessing and augmentation pipeline configuration is essential for enhancing generalization and model reliability, particularly in clinical settings where high sensitivity and specificity are needed [18].

VIII. Conclusion

This study evaluated the effectiveness of three contrast enhancement techniques—contrast stretching, histogram equalization, and adaptive equalization (CLAHE)—in the context of lung mass detection using a YOLOv5-based object detection pipeline trained on chest X-rays. Among the three, adaptive equalization yielded the best baseline results, achieving 80.7% mAP@0.5, 87.3% precision, and 75.8% recall when combined with saturation augmentation. This confirms findings in prior literature that emphasize the utility of CLAHE in enhancing local contrast in radiographic imaging [10], [12].

Subsequent experiments demonstrated that carefully tuned data augmentations such as brightness, exposure, and saturation variations further boost model robustness. Notably, the saturation augmentation produced the highest performance, while exposure and brightness achieved more balanced recall but slightly lower precision. These findings indicate that image manipulation at both preprocessing and augmentation levels plays a pivotal role in overcoming limitations inherent to low-contrast and low-resolution X-ray data.

Despite the relatively small dataset (937 base images, expanded to 1593 with augmentation), the experimental design proved effective for evaluating model sensitivity to contrast and visual diversity. The model showed consistent detection capability even with basic bounding box annotations, suggesting the potential for efficient implementation in real-world clinical settings, particularly in low-resource or mobile deployments where CT or PET scans are unavailable.

However, limitations remain. The model struggles with extremely small lesions and regions with overlapping anatomical features, such as rib intersections and vascular shadows. These false positives and false negatives—analyzed in our Error Analysis section—point toward opportunities for future enhancements. Strategies such as segmentation-guided object detection, attention mechanisms, or ensemble learning could improve sensitivity, especially for subtle pathologies.

Furthermore, while YOLOv5 provided an excellent balance between accuracy and inference speed, emerging architectures such as YOLOv8 or transformer-based detectors may offer improved performance on complex radiographic tasks. Expanding the dataset and incorporating domain-specific knowledge, such as radiologist-labeled severity or 3D multi-view synthesis, may further enhance detection accuracy and clinical applicability.

In summary, this research highlights that a carefully constructed pipeline combining adaptive equalization and saturation-based augmentation enables a YOLOv5 model to approach performance benchmarks traditionally achieved by CT-based models—while using only CXR data. These findings reinforce the value of preprocessing-aware design in deep learning for medical imaging and pave the way for efficient, scalable solutions to support diagnostic workflows in early lung cancer detection.

References

[1] W. H. Organization, "Global cancer statistics," 2022, accessed June 2025. [Online]. Available: https://www.who.int/news-room/fact-sheets/detail/cancer

[2] E. Sogancioglu, B. van Ginneken, and K. G. v. L. Murphy, "Deep learning for chest x-ray analysis: A survey," *arXiv preprint arXiv:2103.08700*, 2021. [Online]. Available: https://arxiv.org/abs/2103.08700

[3] X. Wang, Y. Peng, L. Lu, Z. Lu, M. Bagheri, and R. M. Summers, "Chestx-ray8: Hospital-scale chest x-ray database and benchmarks on weakly-supervised classification and localization of common thorax diseases," *Proceedings of the IEEE Conference on Computer Vision and Pattern Recognition*, pp. 2097–2106, 2017. [Online]. Available: https://openaccess.thecvf.com/content_cvpr_2017/html/Wang_ChestX-ray8_Hospital-Scale_Chest_CVPR_2017_paper.html

[4] P. Rajpurkar, J. Irvin, K. Zhu, B. Yang, H. Mehta, T. Duan, D. Ding, A. Bagul, C. Langlotz, K. Shpanskaya *et al.*, "Chexnet: Radiologist-level pneumonia detection on chest x-rays with deep learning," *arXiv preprint arXiv:1711.05225*, 2017. [Online]. Available: https://arxiv.org/abs/1711.05225

[5] E. Sogancioglu, E. Calli, B. van Ginneken, and K. M. van Leeuwen, "Deep learning for chest x-ray analysis: A survey," *Medical Image Analysis*, vol. 72, p. 102125, 2021. [Online]. Available: https://doi.org/10.1016/j.media.2021.102125

[6] R. Pandey *et al.*, "Yolo advances to its genesis: a decadal and comprehensive review of the you only look once (yolo) series," *Artificial Intelligence Review*, 2025. [Online]. Available: https://link.springer.com/article/10.1007/s10462-025-11253-3

[7] A. Author, "Evaluating pre-processing and deep learning methods in medical imaging: Combined effectiveness across multiple modalities," *Alexandria Engineering Journal*, vol. 119, pp. 558–586, 2025.

[8] M. Chen, Y. Liu, Z. Li *et al.*, "Human-centered explainable ai (xai): Robustness, fairness and bias mitigation," *Nature Machine Intelligence*, vol. 3, pp. 709–719, 2021. [Online]. Available: https://www.nature.com/articles/s42256-021-00414-z

[9] J. Moore, H. Lee, J. Kim, and V. M. Patel, "Bias mitigation in medical imaging: A study on the effect of histogram equalization on chest x-ray datasets," *Scientific Reports*, vol. 12, no. 1, pp. 1–12, 2022. [Online]. Available: https://www.nature.com/articles/s41598-022-05745-6

[10] e. a. Yamashita, "Pulmonary abnormality screening on chest x-rays from different machine specifications: a generalized ai-based image manipulation pipeline," *European Radiology Experimental*, 2023. [Online]. Available: https://eurradiolexp.springeropen.com/articles/10.1186/s41747-023-00386-1

[11] M. Siddhartha and A. Santra, "Covidlite: A depth-wise separable deep neural network with white balance and clahe for detection of covid-19," *arXiv preprint arXiv:2006.13873*, 2020. [Online]. Available: https://arxiv.org/abs/2006.13873

[12] Anonymous, "Hybrid clahe-cnn deep neural networks for classifying lung diseases from x-ray acquisitions," *Electronics (MDPI)*, 2022. [Online]. Available: https://www.mdpi.com/2079-9292/11/19/3075

[13] E. Sogancioglu *et al.*, "Deep learning for chest x-ray analysis: A survey," *arXiv preprint arXiv:2103.08700*, 2021. [Online]. Available: https://arxiv.org/abs/2103.08700

[14] Anonymous, "Enhanced diagnostic accuracy for multiple lung diseases using a fine-tuned mobilenetv2 model with advanced pre-processing techniques," *ScienceDirect*, 2024. [Online]. Available: https://www.sciencedirect.com/science/article/abs/pii/S0957417424021390

[15] H. Al Ewaidat and Y. El Brag, "Identification of lung nodules ct scan using yolov5 based on convolution neural network," *arXiv preprint arXiv:2301.02166*, 2022. [Online]. Available: https://arxiv.org/abs/2301.02166

[16] X. Yang, C. Liu, F. Zhao, and L. Zhang, "Grad-cam++ as a tool for explainability in deep neural networks applied to chest x-ray imaging," *Frontiers in Artificial Intelligence*, 2023. [Online]. Available: https://www.frontiersin.org/articles/10.3389/frai.2023.1140001/full

[17] C. Li, Y. Xu, X. Qian, T. Zhang, and Q. Liu, "Small object detection in medical imaging: A survey and future perspectives," *IEEE Reviews in Biomedical Engineering*, vol. 14, pp. 216–233, 2021. [Online]. Available: https://ieeexplore.ieee.org/document/9218993

[18] Q. V. Nguyen, B. T. Vo, P. T. Nguyen, T. D. Le *et al.*, "Anomalies detection on chest x-ray images using a two-stage yolov5s-frcnn pipeline with cropped lung field detection and transfer learning," *International Journal of Semantic Computing*, vol. 17, no. 1, pp. 1–17, 2023. [Online]. Available: https://www.worldscientific.com/doi/full/10.1142/S2196888823500094